Research on Engineering Structures & Materials
www.jresm.org
Research Group

Research Article

Corrosion and wear behavior of recycled aluminum alloy reinforced with rice husk ash

Olatunji P Abolusoro [*,a], Moshibudi Caroline Khoathane [b], Washington Mhike [c]

Dept. of Chemical, Metallurgical and Materials Eng., Tshwane University of Technology, South Africa

Article Info

Article History:

Received 01 July 2025

Accepted 12 Aug 2025

Keywords:

Aluminum waste cans;
Corrosion;
composite;
Rice husk ash;
Wear

Abstract

Wear and corrosion analysis were performed on recycled aluminum alloy/rice husk ash composites in this study. The composite was prepared by adding rice husk ash (RHA) as reinforcement in percentages of 5, 10 and 15 to aluminum waste cans, as the matrix. The corrosion investigations show that the RHA particles influenced the corrosion characteristics of the composites. The susceptibility to corrosion increases as the percentage addition of the RHA increases beyond 5% wt. The corrosion was mitigated most at 5% wt. reinforcement, while the worst corrosion attack occurred at the 15% wt. of RHA addition. The wear analysis revealed that the RHA addition to the aluminum matrix improved the wear resistance of the composites. The wear rate reduces as the percentage addition of the RHA increases, resulting in the lowest wear rate at 15% wt. of RHA. The improvement in the resistance to wear of the composites indicates an enhancement in the composite's hardness, highlighting the promising potential of integrating RHA into aluminum alloy to promote hardness and resistance to wear. The corrosion analysis, however, indicates that introducing RHA to the aluminum matrix beyond 5% wt. may compromise the application of the composites in corrosive environments unless countermeasures are incorporated.

1. Introduction

Aluminum alloy is among the most widely used alloys for various engineering applications. Its distinctive properties—such as a high strength-to-weight ratio, low melting point, resistance to corrosion, recyclability, and availability—have made it highly valuable to engineers. [1-4]. However, drawbacks like warping at high temperatures, high cost, weldability issues, denting and scratching, and machining challenges have prompted researchers to explore ways to modify aluminum 's properties for specific applications. This has been achieved through reinforcements with ceramic compounds like silicon carbide, boron carbide, titanium carbide, and silicon oxides [5-7]. Some researchers have also investigated nanoparticles [8-10]. These reinforcements are incorporated into the aluminum matrix to form aluminum matrix composites (AMCs). The simplicity, cost-effectiveness, sustainability, and uniform properties of AMCs have attracted considerable research interest. Studies have shown that AMCs often exhibit superior mechanical, thermal, and wear properties compared to pure aluminum. Additional characteristics such as a low thermal expansion coefficient, high-temperature resistance, and good corrosion resistance have also been reported [6, 11-13]. These qualities are highly relevant for engineering applications. Agricultural wastes are increasingly being used as reinforcements in aluminum matrices. Among these are coconut shell ash, palm kernel shell ash, bagasse, bamboo leaf ash, melon shell ash, groundnut shell ash, and rice husk ash [14-16]. Researchers have documented improvements in the mechanical behavior of AMCs reinforced with agricultural wastes [16-18]. Reports on their corrosion and wear behavior—though fewer—have also been published. Rice husk ash (RHA) is

*Corresponding author: abolusoroolatunji@yahoo.com
[a]orcid.org/0000-0003-1493-3445; [b]orcid.org/0000-0002-5328-2721; [c]orcid.org/0000-0003-4670-1171;
DOI: http://dx.doi.org/10.17515/resm2025-995ma0701rs

one of the most prominent agro-wastes gaining attention as a reinforcement for AMCs recently, owing to its composition, which is known to enhance strength in aluminum matrices [19, 20]. Beyond mechanical properties, the wear and corrosion behavior of RHA-reinforced AMCs have also been investigated. Notably, Alaneme et al [11] examined composites with an Al-Mg-Si matrix reinforced with hybrids of SiC and RHA, which revealed inconsistencies in corrosion performance at different reinforcement levels. Kanayo and Olubambi [21] found that the corrosion rate increased as the percentage of RHA increased in Al-Mg-Si matrices. Similarly, Ononiwu et al [22] reported that adding eggshell and fly ash reinforcements could improve corrosion resistance at a 5% reinforcement level. Gouda et al. [23] demonstrated enhanced corrosion resistance in magnesium alloys with a 5% weight addition of eggshells. Despite these reports of improved corrosion resistance at 5% additions of fly ash and eggshells, other findings suggest that reinforcement addition can dismantle the protective oxide layer (Al_2O_3) on the surface of AMCs, making them more susceptible to corrosion attack [22, 24-26]. The formation of intermetallic such as manganese and iron significantly influence the electromechanical performance of AMCs, due to their higher electrode potentials compared to aluminum [24, 27]. Variations in these potentials are known to initiate pitting corrosion in alkaline environments. Additionally, manufacturing processes—including machining, powder metallurgy, and stir casting—have been shown to affect the rate of corrosion [27-29].

Efforts have been made to collect data on material properties for agro-waste-reinforced AMC, and a relatively consistent pattern in mechanical performance has been observed. However, the results concerning corrosion behavior are inconsistent, unlike those for mechanical properties. The conflicting reports on the corrosion behavior of various agro-wastes reinforced AMCs make it difficult to understand and predict their corrosion mechanisms. Therefore, further electrochemical analysis on more agro-waste-reinforced AMCs is necessary, as it will help fulfil some essential assessments to evaluate their performance and suitability in different environments.

The wear assessment of AMCs is very significant for tribological applications. Some researchers have made various attempts to investigate the wear behavior of some agro-waste reinforced composites. Kanayo and Olubambi [21] reported an increase in the wear rate of the Al-Mg-Si matrix reinforced with RHA as the weight additions of the rice husk ash increased. The authors equally reported a blend of adhesive and abrasive wear mechanisms in the composites as the RHA wt.% increases. Alaneme et al [11] in a similar study on a hybrid composite using Al-Mg-Si matrix, Silicon carbide and RHA reinforcements revealed a comparable wear resistance between the matrix and the composite reinforced with only SiC. Another study by Abdulwahab et al [30] shows an enhancement in the wear resistance of melon shell ash reinforced Al-7%Si-0.3%Mg composite as the percentage of melon shell ash addition increases. In another study, Alaneme and Sanusi [31] reinforced an aluminum matrix with graphite, alumina and rice husk ash. They reported that the composites with graphite addition were more resistant to wear although the resistance to wear declined as the graphite addition increased from 0.5% to 1.5%. Mishra et al [32] also reported an enhancement in the wear resistance of aluminum alloy (LM6) reinforced with rice husk ash. Oke et al [33] in a related study also revealed similar findings of wear resistance improvement in an AL-Cu-based alloy reinforced with rice husk ash. Another report from Mustafa et al [34] shows that SiC addition to aluminum matrix improved the resistance to wear and the hardness of the composite significantly, while the RHA addition improves the wear resistance marginally compared to the unreinforced alloy.

The reports available, as reviewed above, on the wear characteristics of AMCs are not sufficient to determine a consistent tribological trend. Therefore, this research effort focuses on the electromechanical behavior of a composite made from recycled aluminum alloy matrix reinforced with rice husk ash. The production of the composite from waste aluminum cans and rice husk ash emanated from the disposal problems these wastes constitute to the environment. The wastes are often discarded indiscriminately and sometimes burned in the air as a means of disposal, thereby polluting the environment and posing health hazards to humans and animals. The conversion of these wastes to lightweight composites would find applications in automobiles for building body panels, structures and interior components and in marine for the construction of Boat hulls, superstructures, propeller blades and interiors. Other areas of applications include sports (Tennis

rackets, helmets and bicycle frames), energy (wind turbine blades), and the military (armour carriers and drones). These applications will ameliorate the problem of managing these wastes and make the environment safer.

The tribological and electrochemical study on the composite will further improve the knowledge base of agro-waste-reinforced AMCs and their applications in marine environments and other environments susceptible to corrosion and mechanical degradation. This study would also guide the selection of the appropriate reinforcement level to enhance the lifespan and reliability of the composites.

2. Materials and Methods

2.1 Preparation of Rice Husk Ash and Aluminum Cans

The waste cans were acquired from dumpsites at different locations in Nigeria (Fig. 1 a). They were thoroughly washed and manually crushed. The rice husk was acquired from a local rice mill, washed to get rid of the dirt and impurities, sun-dried and then burnt in a ceramic container placed in a furnace at 600 °C for 10 hours. The obtained ash was sieved with a 38 μm sieve to obtain the reinforcement (Fig. 1 b). The chemical composition analysis carried out on the waste cans is presented in Table 1[35] while the X-ray fluorescent (XRF) investigation on the rice husk ash is given in Table 2 [36].

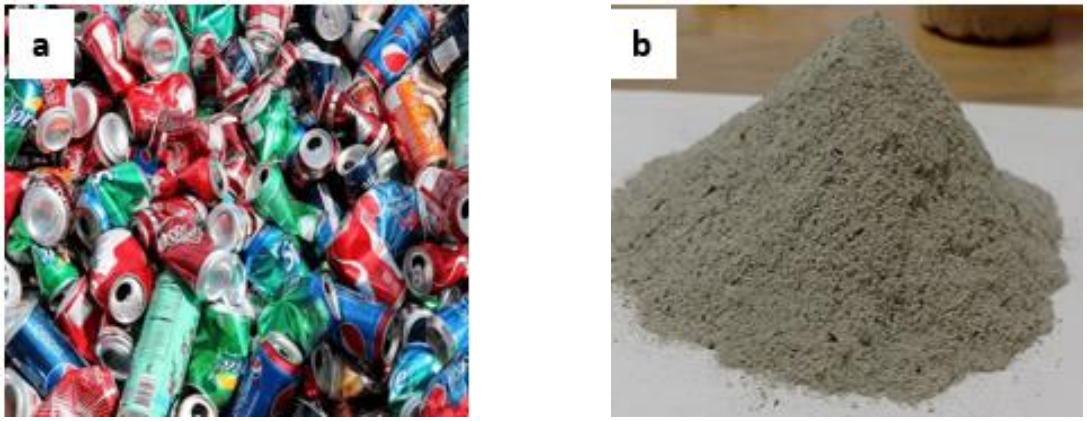

Fig. 1. (a) Aluminum waste cans, (b) rice husk ash

Table 1. Compositional analysis of the Aluminum waste cans

Element	Fe	Mn	Ti	K	Si	Cu	Zn	Mg	Cr	Al	Others
% Wt	0.431	0.388	0.006	0.013	0.59	0.074	0.194	2.143	0.008	96.043	0.11

Table 2. Composition of the RHA

Oxides	Al_2O_3	SiO_2	MgO	Na_2O	CaO	K_2O	MnO	TiO_2	P_2O_5
Weight %	0.80	75.81	3.74	1.58	1.39	2.52	0.01	0.05	11.29
Oxides	Fe_2O_3	S	Cl	ZnO	TiO	CuO	ZrO_2	BaO	ThO_2
Weight %	0.87	0.56	0.23	0.05	0.03	0.01	0.01	0.11	0.01

2.2 Composite Preparation

The compressed Aluminum waste cans were loaded in a crucible and fed into a pre-heated furnace at 500 ^{0}C. The furnace temperature was raised to 720^o C and the waste cans were soaked at that temperature for about 45 minutes for complete melting. The crucible was brought out of the furnace, and the slags and impurities were removed from the molten aluminum. The rice husk ash

was introduced into the molten aluminum alloy in percentages of 0%, 5%, 10%, and 15% and reheated for 15 minutes in the furnace before pouring it into the prepared mould. The 0% is the unreinforced (control) sample.

2.3 Wear Test

Three samples for each wear test were cut from the composites into 10mm × 30mm. They were mounted, grinded and polished to obtain a mirror surface, after which they were weighed before commencing the wear tests. A tribometer (RTEC Multifunctional) furnished with MFT17 software and an alloy steel ball of diameter 6.30mm was utilized for the testing. A 20N load at a sliding speed and distance of 3 mm/s and 3 mm, respectively, were applied for 360 seconds on the samples at ambient temperature following the ASTM G99-95 standard. The wear surfaces were examined with a scanning electron microscope (SEM).

2.4 Corrosion test

The samples, measured 12 mm × 4 mm each, were cut from the composites for the corrosion tests. The samples were mounted, grinded and polished to mirror surfaces. The samples were coated with paint, leaving about 1.00 cm^2 exposed to the electrolyte. The corrosive medium is a 3.5% wt. sodium chloride at ambient temperature. Three conventional electrode cell arrangements were used for the electrochemical measurement. The counter electrode is a platinum wire, while the reference electrode is a non-aqueous Ag/AgCl. The potentials of the composite were determined using a PGSTAT302N potentiostat equipped with NOVA software version 1.8. The samples were immersed in the electrolyte for an hour to achieve a stable open-circuit potential (OCP). The potentiodynamic potential range of -50 to +50 mV at a scan rate of 0.125 mV/s was selected for the test. Three samples were tested for the corrosion.

3. Results and Discussion

3.1 Corrosion Analysis

3.1.1. Potentiodynamic polarization analysis

The resulting potentiodynamic polarization curve from the corrosion test is shown in Fig. 2. The curves show distinct features at each percentage weight addition of the reinforcement. The potentiodynamic polarization curves for the four samples gave the data presented in Table 3.

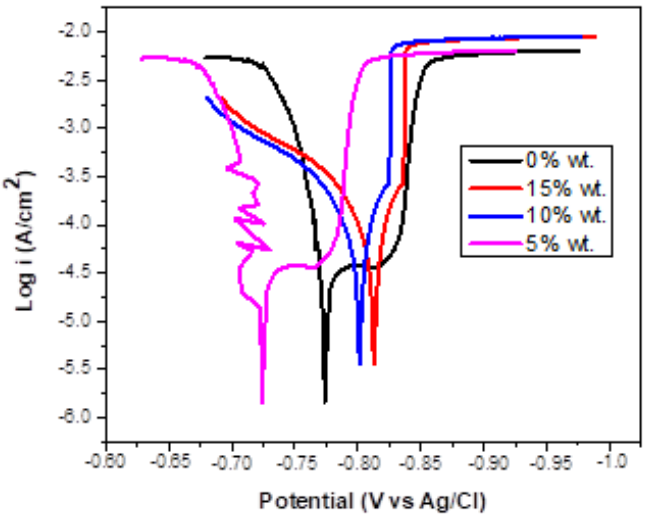

Fig. 2. Potentiodynamic polarization curves of the composites

The information obtained from the polarization analysis, as shown in Table 3, revealed that adding RHA to recycled aluminum altered the corrosion properties of the composites. The corrosion current (Icorr), shown in Fig. 3, decreased slightly at 5% addition but rose marginally at 10% wt and increased further at 15% wt. This indicates that higher RHA particle content leads to increased

corrosion. The electrochemical corrosion potential (Ecorr) of pure aluminum, i.e., 0% wt, suggests a moderate corrosion tendency, typical of aluminum alloys. The Ecorr became more negative with 5% wt addition, indicating reduced electrochemical activity on the surface of the composite. However, at 10% wt and 15% wt, the Ecorr increased again, showing a stronger corrosion tendency at higher reinforcement levels. The corrosion rate (mm/year), which measures material loss caused by corrosion over time, was 1.3207×10^{-3} mm/year for unreinforced aluminum. It decreased to 1.2170×10^{-3} mm/year at 5% addition, then rose to 1.5068×10^{-3} mm/year at 10%, and further to 1.7180×10^{-3} mm/year at 15% wt, representing the highest corrosion rate observed, as shown in Fig. 4. The corrosion rate increases as RHA addition exceeds 5% wt. Similar findings were reported by Kanayo and Olubambi [21] and Ononiwu et al. [22].

Table 3. Potentiodynamic polarization data

%Wt.	I_{corr} (μA/cm²)	E_{corr} (V)	R_{ct} (ohms)	Corrosion Rate (mm/year) × 10^{-3}
0	1.1366	-0.78706	22854	1.3207
5	1.0473	-0.72526	30219	1.2170
10	1.2967	-0.80864	18498	1.5068
15	1.6500	-0.81905	17719	1.7180

The observed trend in corrosion behavior could be linked to variations in RHA particle content in the aluminum matrix. Corrosion was most effectively mitigated at 5% wt, possibly due to the even distribution of RHA particles within the matrix, which acts as a barrier to corrosion and promotes the formation of passive oxide layers on the composite surface. At 5%, the evenly distributed RHA might also reduce the active surface area exposed to the corrosive medium, lowering susceptibility to corrosion and stabilizing passive oxide layers. Higher corrosion attack at 10% and 15% wt could be due to the larger quantities of reinforcement, leading to uneven distribution, agglomeration, interfacial defects, and porosity [14, 36]. These factors create micro-galvanic sites and crack initiation points, disrupting the formation of passive layers and making the composites more vulnerable to corrosion [37, 38]. Another possible reason for the increased corrosion rates at these higher RHA percentages is the metallic content of the RHA itself. This can promote the formation of intermetallic compounds that inhibit the protective actions of the passive layer [23, 39].

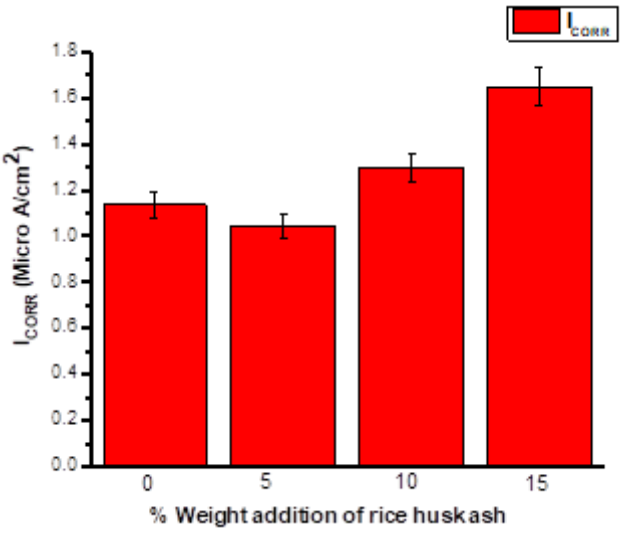

Fig. 3. Corrosion current at different weight additions of RHA

These intermetallic are often thought to form from the combination of aluminum with elements such as Cu, Fe, Mg, Mn, Zn, and Si present in the RHA and incorporated into the aluminum matrix during casting. Although the precise characteristics of the phases—including size, composition, distribution, and electrochemical properties—have not been quantitatively detailed in this study, previous research shows that they significantly influence the corrosion mechanisms of aluminum

composites [40]. It is plausible that they act as cathodes or anodes relative to the aluminum matrix to form micro-galvanic coupling and initiate pits and localized corrosion. Additionally, chloride ions may preferentially concentrate near the intermetallic, potentially disrupting the uniformity of the passive oxide film and accelerating localized attack [41, 42]. The electrochemical difference between the aluminum matrix and the intermetallic could sustain the growth of pits once formed [39, 40].

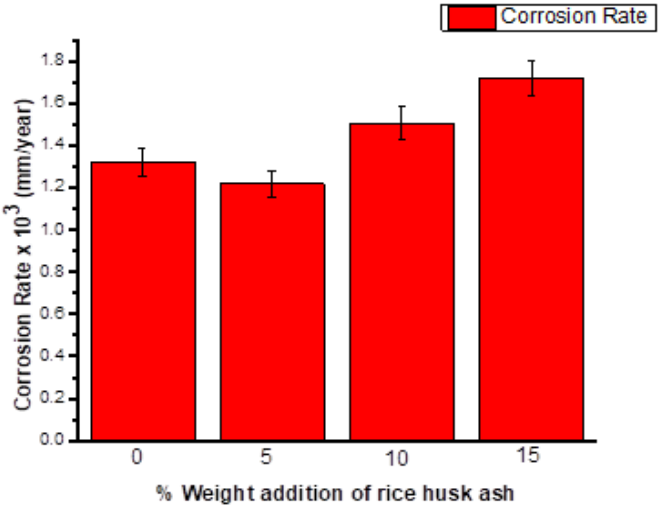

Fig. 4. The corrosion rate at different weight additions of RHA

3.1.2. Scanning Electron Microscope (SEM) Examination of The Corroded Surfaces

The SEM examinations carried out on the corrosion-tested samples are presented in Fig. 5. The surfaces demonstrate clusters of localized pitting corrosion that could be attributed to the occurrence of localized variations in the electrochemical potentials of the composites. There were pit formations on the surfaces of the samples, indicating that the passive film (Al2O3) on the composites was insufficient to mitigate the influence of halide ions (Cl^-) [22, 23, 41]. There was little pitting corrosion attack in Figs. 5 a and b, representing 0% wt. and 5% wt. respectively. There was no evidence of major pits or deep cavities in the 5% wt (Fig. 5b) owing to strong interfacial bonding of the RHA and the matrix, which reduces crevices and galvanic corrosion. However, more pits could be observed in Fig. 5c and d, representing 10% wt. and 15% wt. of RHA, with signs of aggressive attack in some areas. The pitting corrosion attack could be attributed to poor distribution and agglomeration of RHA particles, which might have led to micro-galvanic cells formation between the matrix and the RHA. This results in more corrosion attacks suffered by the composites at those reinforcement additions. As revealed by the EDS, the presence of elements such as iron, manganese, and silicon, which are known for their corrosive aggressiveness and possess a higher electrode potential than aluminum, creates galvanic sites to initiate corrosion. The EDS of the corroded samples also revealed the occurrence of Chlorine (Cl), Manganese (Mn), Oxygen (O), Iron (Fe) and other elements. These elements create intermetallic compounds known to advance corrosion attack in aluminum composites [43]. The EDS elemental mappings as shown in Fig. 5b at the 5% wt. revealed the highest aluminum retention of 55.3 % and the lowest percentages of Cl (0.8 %) and O (1.2 %). This is an indication that the sample suffered the least corrosion attack when compared to the other samples. The sample at the 15% wt. (Fig. 5d) has the lowest aluminum retention of 52.9 % and the highest O and Cl content of (6.7 %) and (1.8 %) respectively. The reduced presence of the Al suggests surface corrosion and loss of Al to form part of the corrosion products through oxidation and pitting. The high chloride ion breaks the oxide film on the composite's surface, causing localized disintegration and pitting corrosion [44-46]. This sample experienced the highest corrosion attack, as evidenced in the corrosion rates of all the samples presented in Fig. 4. Other elements such as Fe, Si and Mn observed in the EDS spectra emanate from the composition of the RHA. However, Na suggested residual salt deposits from NaCl. Sodium ions predominantly aggregate in corrosion pits or on the oxide layer following the evaporation of the electrolyte [47, 48].

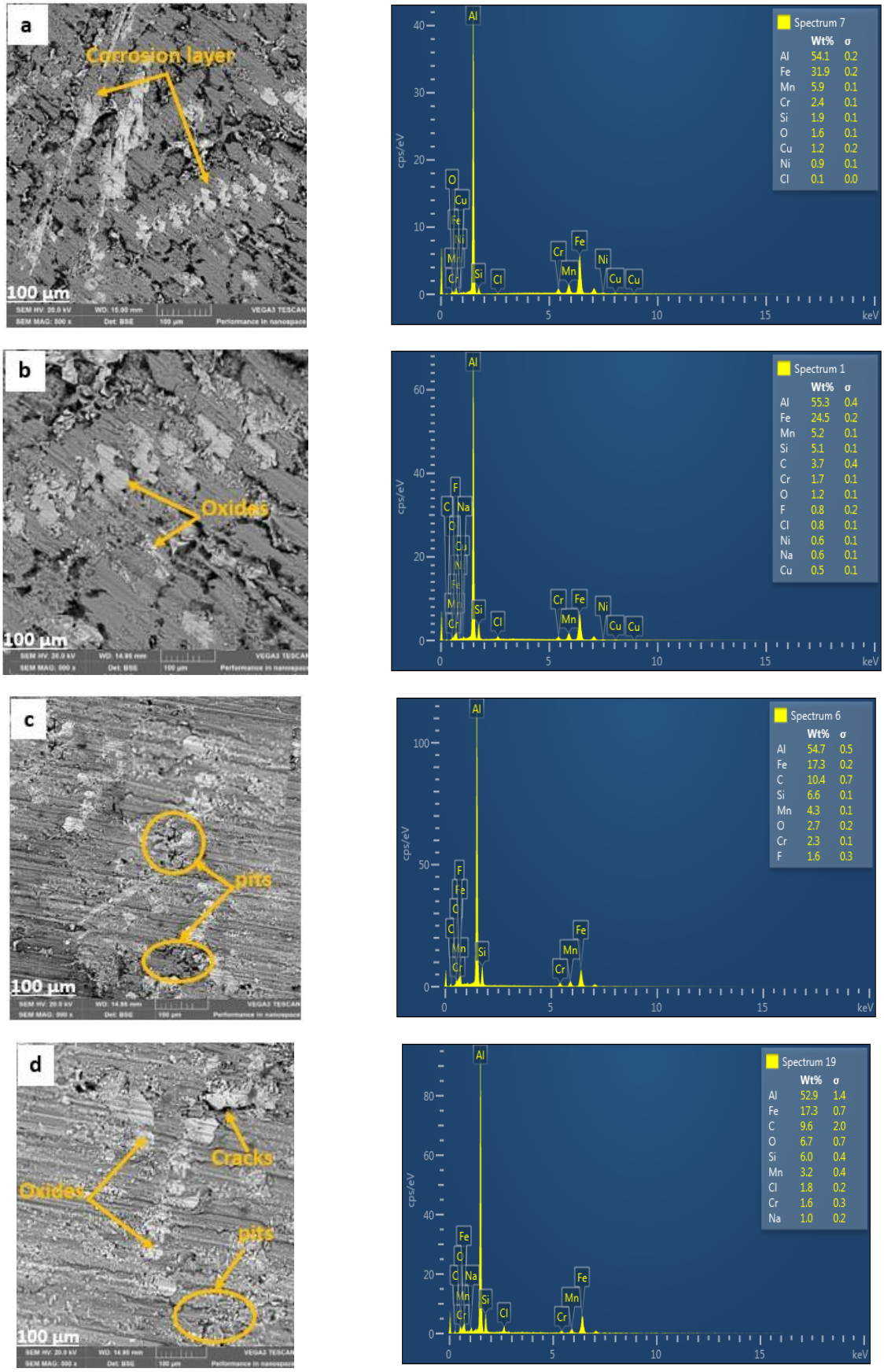

Fig. 5. SEM and EDS images of the corroded surfaces showing pitting corrosion sites, oxide formation and the elemental compositions. (a) Sample at 0% Wt. of RHA (b) Sample at 5% Wt. of RHA (c) Sample at 10% Wt. of RHA (d) Sample at 15% Wt. of RHA

3.2 Wear Characteristics

The coefficient of friction and wear depth were generated by the MFTI7 software of the tribometer, while the wear rate was calculated using equation (1) [49].

$$Wear\ rate\ (mm^3/Nm) = \frac{Wear\ volume}{Applied\ force \times Sliding\ distance} \times 100 \quad (1)$$

3.2.1 Coefficient of Friction and Wear

The coefficient of friction (COF) responses of the samples is shown in Fig. 6, while the average COF of the samples is depicted in Fig. 7, and the wear rate is illustrated in Fig. 8. The responses of the samples as presented in Fig. 6 revealed that the RHA impact the wear behavior of the composites, especially at higher additions of reinforcements.

The average COF, as shown in Fig. 7, shows a systematic and significant decrease as the reinforcement additions increase from the initial 5% to 15%. A drastic reduction in the COF was noticed at 10% and 15% rice husk ash additions, representing 74% and 76% respectively, lower than the COF of the control samples. The implication of this is that the rice husk addition behaves as a solid lubricant, helping to lower the metal-to-metal contact, thereby decreasing friction. Rice husk ash, as shown in Table 2, is rich in silica, which is inherently hard and could also help in lowering the metal-to-metal contacts, resulting to wear reduction.

Table 4. Summary of the mechanical properties of the composites at different reinforcement levels [36]

Weight %	Tensile (MPa)	Hardness (BHN)	Impact Energy (J)
0	93.0	47.0	75.0
5	101.3	52.5	77.0
10	121.6	55.5	81.5
15	111.6	70.2	96.0

The wear rate (Fig. 8) also follows the same trend as the COF. The wear rate decreases as the percentage weight additions increase. The rice husk ash reduces the wear rate of the composite from 5.6×10^{-4} mm^3Nm^{-1} of the unreinforced alloy to 2.3×10^{-4} mm^3Nm^{-1}, representing a 59% reduction at the 15% RHA addition. This behavior could be linked to the presence of known hard compounds in the RHA, which include MgO, $Al2O_3$, CaO, TiO_2, Fe_2O_3, and SiO_2. These compounds impact the hardness of the matrix, promoting its resistance to localized plastic deformation, thereby lowering the wear rate [33, 36]. Reduction in wear rate is usually correlated with improvement in hardness. The wear rate reduction of the composites agreed with the earlier reports on the enhancement of hardness and other mechanical properties of the composites, as presented in Table 4. The inclusion of the RHA improves the surface hardness of the composites, leading to a reduction in the real contact area and a resulting decrease in frictional force. This translates to less adhesion and deformation during the sliding. The low wear rate obtained at higher reinforcement addition could also be due to the reduction in adhesion and ploughing friction of the composites. Pure aluminum alloy usually demonstrates adhesive wear and high COF as a result of material transfer and sticking [50, 51]. The adhesion becomes minimized with the addition of the RHA to the alloy. The RHA interrupt the matrix continuity, lowering the frictional drag and welding, thereby reducing the wear rate [52, 53]. The RHA addition to the matrix, especially at 10% and 15% contributed to the development of protective tribo-layers from wear debris. These layers could serve as third-body lubricants, reducing direct asperity contact, leading to a lowering of the COF and the wear rate.

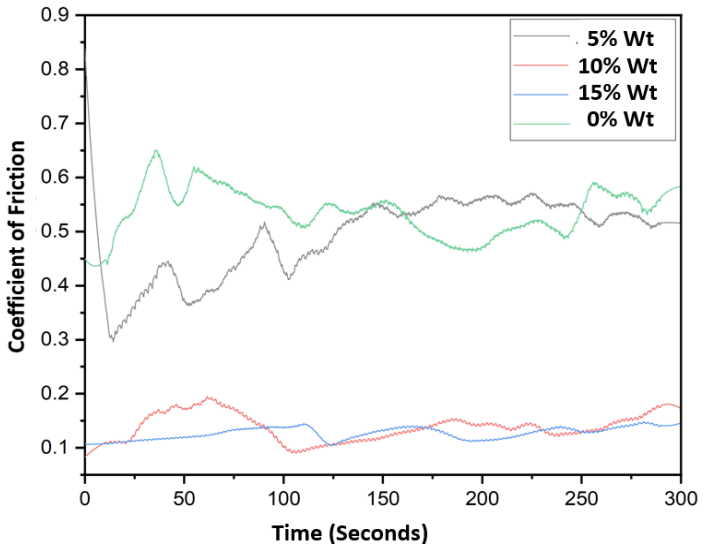

Fig. 6. COF responses at various weight additions of RHA

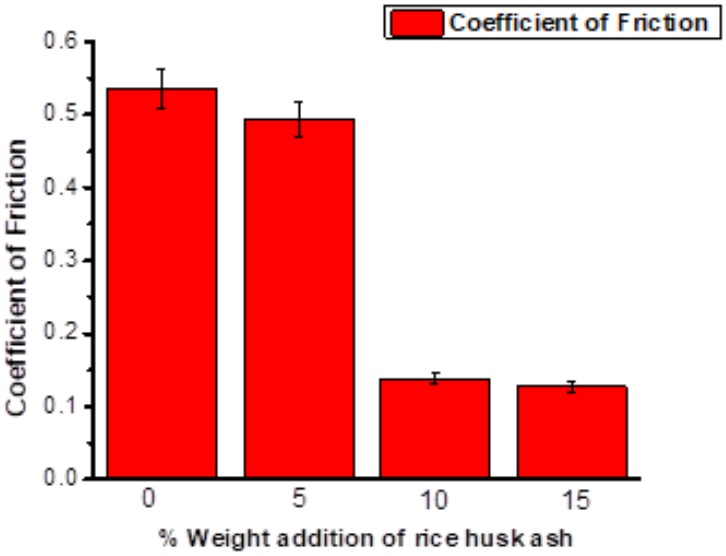

Fig. 7. Average coefficient of friction at different weight additions of RHA

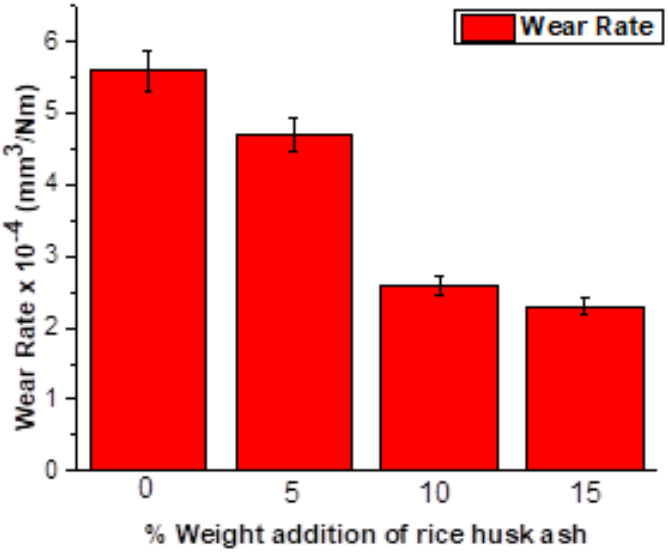

Fig. 8. The wear rate at different weight additions of RHA

3.2.2 SEM and Wear Tracks Analysis

The wear tracks of the samples were studied with SEM and presented in Fig. 9. A wide range of abrasion marks could be noticed on the surfaces of all the samples, suggesting that the material removal processes comprise micro-cutting and microchipping. The unreinforced sample, i.e 0% wt. shown in Fig. 9a exhibits severely scratched, fairly long and ploughing trenches resulting in a high material removal rate, as earlier reported in section 3.2.1 and a larger plastic deformation owing to the softer α-Al matrix. At the 5% RHA addition (Fig. 9b), the wear tracks are a little narrower with a slight drop-in material removal rate. This indicates lower adhesive wear and a slight enhancement in load-bearing capacity of the composite at that RHA addition. At 10% RHA addition (Fig. 9c), fewer cracks with narrower and smoother wear tracks are noticeable. A similar scenario could be observed at the 15% wt. in Fig. 9d, where the wear tracks remain narrower with minimized material removal rate.

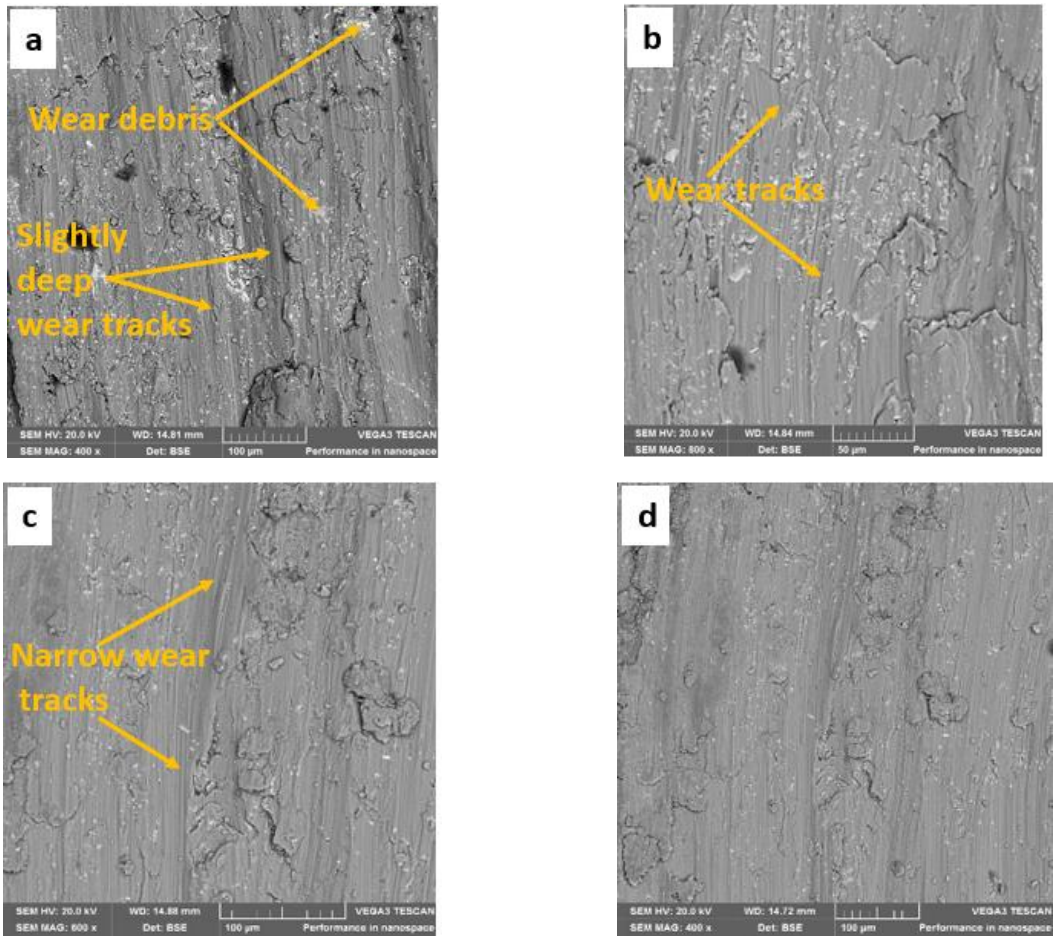

Fig. 9. SEM analysis of the wear samples showing the wear tracks and debris. (a) Sample at 0% Wt. of RHA (b) Sample at 5% Wt. of RHA (c) Sample at 10% Wt. of RHA (d) Sample at 15% Wt. of RHA

The morphological observation of the wear tracks generally indicates that more material removal occurs in the unreinforced alloy than in the composites. The RHA advanced the intermetallic particulate bonding of the composites, thereby narrowing the wear grooves along the lines of deformation. The groove edges of the composites show little plastic deformation with shallow cuts compared to the pure alloy. Abdulwahab et al [30] and Shanmughasundaram and Subramanian [54] reported a similar finding.

3.3 Statistical Analysis of The Corrosion and Wear Data

3.3.1. Statistical Summary

A brief statistical analysis of the corrosion and wear studies is shown in Table 5. The average corrosion current and corrosion rate are slightly higher than those of the unreinforced alloy, while the average COF and wear rates were found to be lower than those of the unreinforced aluminum. These confirmed the influence of RHA on the corrosion susceptibility and wear resistance of the composites. The standard deviations indicate low variability across the various reinforcement levels, suggesting that the RHA influences the rate of degradation of the composites. The low standard deviation across the measured values also demonstrates the predictability and reliability of the performance. The small error bars indicate that the sample data are closely clustered around the mean, suggesting good measurement reliability.

Table 5. Statistical summary of the wear and corrosion studies

	Mean	Standard deviation	Error bar
Corrosion current	1.283	0.266	0.133
Corrosion rate	1.441	0.220	0.110
Coefficient of friction	0.323	0.212	0.111
Wear rate	3.800	1.460	0.803

3.3.2 ANOVA

Analysis of variance was used to assess the statistical significance of the mean corrosion and wear rates for the four reinforcement levels of the RHA. The wear and corrosion rates obtained for each reinforcement level are shown in Table 6.

Table 6. Corrosion and wear rates at different percentages of reinforcement

Wt. %	0	0	0	5	5	5
Corrosion rate $\times 10^{-3}$ (mm/year)	1.4011	1.3100	1.2510	1.2211	1.3020	1.1340
Wear rate$\times 10^{-4}$ (mm^3 Nm^{-1})	5.8	6.3	4.9	5.3	3.9	4.9
Wt. %	10	10	10	15	15	15
Corrosion rate $\times 10^{-3}$ (mm/year)	1.5067	1.4459	1.5680	1.8032	1.7142	1.6336
Wear rate$\times 10^{-4}$ (mm^3Nm^{-1})	2.8	3.1	1.8	2.6	2.2	2.1

Table 7. ANOVA for corrosion rate

	Sum of squares (SS)	df	MS	F- Values	P-Values	F Critical
Between group	220.2762	1	220.2762	12.90634	0.00162	4.30095
Within group	375.4802	22	17.06728			
Total	595.7564	23				

The ANOVA for the corrosion rate is presented in Table 7. The null hypothesis states that there is no difference between the means of the groups, while the alternative hypothesis suggests that a difference exists. The variance (F) between the groups is 12.90634, which exceeds 4.30095, the critical variance (F critical), leading to the rejection of the null hypothesis. The P value is 0.000162, which is less than 0.05, the significance level. This also indicates the rejection of the null hypothesis and confirms that at a 95% confidence level, there is a significant difference in the corrosion rate

among the various RHA reinforcement additions. This demonstrates that the RHA percentage addition significantly influenced the corrosion properties of the composites.

The analysis of variance for the wear rate is shown in Table 8. The F value exceeds the F critical value indicating the null hypothesis should be rejected. The probability (P) value is less than the significant level, demonstrating that at a 95% confidence level, there is a significant difference in the wear rate among the different RHA reinforcement additions. This further suggests that the percentage weight additions of RHA equally influence the wear behavior of the composites significantly.

Table 8. ANOVA for wear rate

	Sum of squares (SS)	df	MS	F- Values	P-Values	F Critical
Between group	81.77042	1	81.77042	4.471559	0.046027	4.30095
Within group	402.3092	22	18.28678			
Total	484.0796	23				

3.4 Wear vs Corrosion Performance

The improvement in wear resistance of the composite highlights the importance of incorporating RHA into the aluminum matrix. However, the decrease in corrosion performance of the composites at higher RHA additions could limit their suitability in corrosive environments. The 5% wt. addition of RHA enhances both wear and corrosion resistance and could be the ideal choice for applications requiring significant resistance to electromechanical degradation. Introducing RHA into the aluminum matrix beyond 5% wt. would improve mechanical properties and wear resistance, but where corrosion attack becomes a concern, measures such as inhibitors and coatings can be added to achieve a balance.

3.5 Sustainability and economic impact

The utilization of RHA as reinforcement on recycled aluminum alloys to produce composites offers notable environmental and economic benefits. The aluminum waste cans employed in this study are considerably cheaper than primary aluminum, owing to the lesser energy required for remelting. The rice husk is an abundant and cheaper agro-industrial by-product requiring minimal processing. Reinforcing an aluminum matrix with 5-15 wt.% of RHA can proportionally reduce material costs, thereby saving a significant amount of money in large-scale production and possibly offering incentives for waste diversion. Environmental impact is significantly reduced because recycling aluminum requires less processing energy. Moreover, the demand for rice husk ash in this process prevents the waste from being burnt or landfilled, thereby encouraging circular resource use and reducing methane and other harmful particulate emissions into the atmosphere. The availability and low cost of these materials make their use sustainable.

3.6. Limitations and Future Perspectives

The potentiodynamic test used in this study provides short-term accelerated corrosion data with a simulated electrolyte. The results may not fully represent the real-world corrosion performance of the composites. Also, the study could not include phase analysis of the corroded surfaces through XRD. The wear test used a simplified contact geometry and controlled loading in a dry and non-representative environment, overlooking complex wear modes, debris effects, lubrication and corrosion.

Future research should examine a long-term corrosion assessment of the composites. Fatigue corrosion interaction and phase analysis using XRD could also be explored for a better understanding of the durability of the RHA-reinforced composites. Tribocorrosion study of the composite in future research would better reveal the electromechanical degradation mechanism.

4. Conclusion

The study of the corrosion and wear characteristics of the composite made from recycled aluminum alloy matrix with RHA as reinforcement gave the following conclusion.

- The composites demonstrate higher corrosion rates than the unreinforced alloy, except at 5% RHA addition, where the least corrosion rate of 1.2170 $\times 10^{-3}$ mm/year occurred. The corrosion attack was more severe at higher RHA additions, with the 10% additions having a corrosion rate of 1.5068 $\times 10^{-3}$ mm/year while the 15% addition had 1.7180 $\times 10^{-3}$ mm/year. The improvement in corrosion at 5% RHA addition could be due to the evenly dispersed RHA in the matrix, which acts as a barrier to corrosion attack. The RHA reduces the active surface area of the composites exposed to the corrosive medium, thereby lowering the corrosion susceptibility. It also enhances the formation and stabilization of the passive oxide layers, which inhibit corrosion attack. However, at 10% and 15% RHA additions, inhomogeneous spread of the RHA particle, agglomeration, interfacial defects, and porosity might have occurred. These create micro-galvanic sites and initiate crack points, which disrupt the formation of passive layers on the composite's surfaces, making them more susceptible to corrosion attack. The increase in elements such as iron, magnesium, and silicon in the composites occasioned by high volume addition of the RHA could also advance corrosion attack. These elements inhibit the protective passive layer covering the composites due to their higher electrochemical potential than the pure aluminum. The SEM analysis generally revealed localized pitting corrosion attack, while the EDS of the samples shows the occurrence of Iron, Oxygen and Chlorine, among others, which are known elements accountable for corrosion attack in composites of Aluminum.
- The corrosion rates observed for the composites are relatively low in absolute terms; however, they are substantial enough to influence their suitability for certain industrial applications, particularly in environments that demand durability. Introducing RHA into the aluminum matrix beyond 5% wt. may reduce the utility of the composites in corrosive environments unless measures such as inhibitors and coatings are employed as countermeasures.
- The introduction of the RHA particles to the aluminum matrix improves the wear resistance considerably, as the COF and wear rates were found to be lower than those of the pure alloy. The wear rate decreases as the percentage addition of the RHA to the matrix increases. This leads to the lowest wear rate of 2.3 × 10^{-4} mm^3/ Nm occurring at the 15% wt. whereas the highest wear rate of 5.6 × 10^{-4} mm^3/ Nm was obtained at the unreinforced alloy. The hard metallic contents of the RHA promote interfacial bonding with the matrix, leading to better hardness and more resistance to plastic deformation and wear. The RHA contributed to the development of protective tribo-layers from wear debris. These layers could act as third-body lubricants, reducing direct asperity contact, thereby lowering the COF and the wear rate.
- The better resistance to wear demonstrated by the composites over the unreinforced alloy highlights the great prospect of incorporating RHA into aluminum alloys to improve hardness and resistance to mechanical degradation.
- The statistical analysis of the wear and corrosion rates demonstrates that the RHA additions to the matrix significantly influence the electromechanical behavior of the composites.
- The outcome of this study could help establish the optimal additive concentrations of RHA in aluminum alloys, which would enhance the durability, safety, and performance of the composites. The corrosion and wear data obtained could support further experimental and computational investigations.

References

[1] Khelge S, Kumar V, Shetty V, Kumaraswamy J. Effect of reinforcement particles on the mechanical and wear properties of aluminum alloy composites: Review. In: Materials Today: Proceedings. Elsevier Ltd, 2022; 571-576. https://doi.org/10.1016/j.matpr.2021.09.525

[2] Georgantzia E, Gkantou M, Kamaris GS. Aluminium alloys as structural material: A review of research. Engineering Structures. 2021 Jan;227:111372. https://doi.org/10.1016/j.engstruct.2020.111372

[3] Abolusoro OP, Akinlabi ET. Tribocorrosion Measurements and Behavior in Aluminum Alloys: An Overview. Journal of Bio and Tribocorrosion, 2020; 6:1-13. https://doi.org/10.1007/s40735-020-00393-4
[4] Abolusoro OP, Akinlabi ET. Wear and corrosion behavior of friction stir welded aluminum alloys- An overview. International Journal of Mechanical and Production Engineering Research and Development, 2019; 9:967-982.
[5] Baisane VP, Sable YS, Dhobe MM, Sonawane PM. Recent development and challenges in processing of ceramics reinforced Al matrix composite through stir casting process. International Journal of Engineering and Applied Science 2015; 2:2394-3661
[6] Ikubanni PP, Oki M, Adekunle AA. A review of ceramic/bio-based hybrid reinforced aluminum matrix composites. Cogent Engineering, 2020; 7:1727167. https://doi.org/10.1080/23311916.2020.1727167
[7] Sharma AK, Bhandari R, Pinca-Bretotean C. Impact of silicon carbide reinforcement on characteristics of aluminum metal matrix composite. In: Journal of Physics: Conference Series. IOP Publishing Ltd 2021. https://doi.org/10.1088/1742-6596/1781/1/012031
[8] Kumar S et al. Advantages and Disadvantages of Metal Nanoparticles. In: Tiwari, S.K., Kumar, V., Thomas, S. (eds) Nanoparticles Reinforced Metal Nanocomposites. Springer, Singapore 2023; 978-981. https://doi.org/10.1007/978-981-19-9729-7_7
[9] Rocha F, Simões S. Aluminum Nanocomposites Reinforced with Al2O3 Nanoparticles: Synthesis, Structure, and Properties. J Compos Sci. 2024 Jan 17;8(1):33. https://doi.org/10.3390/jcs8010033
[10] Kumawat, YK, Sehgal, R, Ayoub I, Sehgal R, Kumar V. Recent Progress in the Development of Metallic Composite for Advanced Technologies. In: Tiwari, S.K., Kumar, V., Thomas, S. (eds) Nanoparticles Reinforced Metal Nanocomposites. Springer, Singapore, 2023. https://doi.org/10.1007/978-981-19-9729-7_3
[11] Alaneme KK, Adewale TM, Olubambi PA. Corrosion and wear behavior of Al-Mg-Si alloy matrix hybrid composites reinforced with rice husk ash and silicon carbide. Journal of Materials Research and Technology, 2014; 3:9-16. https://doi.org/10.1016/j.jmrt.2013.10.008
[12] Kar A, Sharma A, Kumar S. A Critical Review on Recent Advancements in Aluminium-Based Metal Matrix Composites. Crystals. 2024 Apr 28;14(5):412. https://doi.org/10.3390/cryst14050412
[13] Singh H, Singh K, Vardhan S, Mohan S, Singh V. A comprehensive review of aluminium matrix composite reinforcement and fabrication methodologies. Funct Compos Struct. 2021 Mar 1;3(1):015007. https://doi.org/10.1088/2631-6331/abddc8
[14] Abolusoro OP, Khoathane MC, Mhike W. Influence of melon shell ash reinforcement on the mechanical and microstructural characteristics of recycled aluminum matrix composites. Research on Engineering Structures and Materials. 2025; 11(2): 783-798. http://dx.doi.org/10.17515/resm2024.320me0614rs
[15] Joseph OO, Kunle OB. Agricultural waste as a reinforcement particulate for Al metal matrix composites (AMMCs). Rev MDPI Fibres, 2019; 7:7-33. https://doi.org/10.3390/fib7040033
[16]Taylor P. Development of metal-matrix composites from industrial/agricultural waste materials and their derivatives- Critical Review. Environmental Science Technology, 2016; 46:143-208. https://doi.org/10.1080/10643389.2015.1077067
[17] Kulkarni PP, Siddeswarappa B, Kumar KSH. A survey on effect of agro-waste ash as reinforcement on aluminum base metal matrix composites. Open Journal of Composite Materials. 2019; 9:12-26. https://doi.org/10.4236/ojcm.2019.93019
[18] Jagannath V, Harish K. Fly ash, rice husk ash as reinforcement with aluminum metal matrix composite: A review of technique, parameter and outcome. ICAPIE 2019; 953-962
[19] Masoumeh K, Naser F, Martin IP, Asadollah A. Rice Husk at a Glance: From Agro-Industrial to Modern Applications. Rice Science, 2024; 31:14-32. https://doi.org/10.1016/j.rsci.2023.08.005
[20] Dixit P, Suhane A. Aluminum metal matrix composites reinforced with rice husk ash: A review. In: Materials Today: Proceedings. Elsevier Ltd, pp 2022; 4194-4201. https://doi.org/10.1016/j.matpr.2022.04.711
[21] Kanayo K, Olubambi PA. Corrosion and wear behavior of rice husk ash - Alumina reinforced Al - Mg - Si alloy matrix hybrid composites. Journal of Materials Research and Technology, 2013; 2:188-194. https://doi.org/10.1016/j.jmrt.2013.02.005
[22] Ononiwu N, Ozoegwu C, Madushele N, Akinribide OJ. Mechanical Properties, Tribology and Electrochemical Studies of Al / Fly Ash / Eggshell Aluminum Matrix Composite. Biointerface Research in Applied Chemistry, 2022; 12:4900-4919. https://doi.org/10.33263/BRIAC124.49004919
[23] Gouda MK, Salman S, Elsayed A. The Effect of Eggshell as a Reinforcement on the Mechanical and Corrosion Properties of MG-ZN-MN Matrix Composite. Acta Metallurgica Slovaca 2021; 27:180-184. https://doi.org/10.36547/ams.27.4.1088
[24] Omoniyi P, Abolusoro O, Olorunpomi O, Ajiboye T, Adewuyi O, Aransiola O, et al. Corrosion Properties of Aluminum Alloy Reinforced with Wood Particles. J Compos Sci. 2022 Jun 28;6(7):189. https://doi.org/10.3390/jcs6070189

[25] Meignanamoorthy M, Ravichandran M, Mohanavel V, Afzal A, Sathish T, Alamri S, et al. Microstructure, Mechanical Properties, and Corrosion Behavior of Boron Carbide Reinforced Aluminum Alloy (Al-Fe-Si-Zn-Cu) Matrix Composites Produced via Powder Metallurgy Route. Materials. 2021 Aug 2;14(15):4315. https://doi.org/10.3390/ma14154315
[26] Bandil K, Vashisth H, Kumar S, Verma L, Jamwal A, Kumar D, Singh N, Sadasivuni KK, Gupta P. Microstructural, mechanical and corrosion behavior of Al-Si alloy reinforced with SiC metal matrix composite, 2021; 53:4215-4223. https://doi.org/10.1177/0021998319856679
[27] Abolusoro OP, Khoathane MC, Mhike W, Omoniyi P, Kailas S V., Akinlabi ET. Influence of welding parameters and post-weld heat treatment on mechanical, microstructures and corrosion behavior of friction stir welded aluminum alloys. Journal of Materials Research and Technology, 2024; 32:634-648. https://doi.org/10.1016/j.jmrt.2024.07.175
[28] Pérez OR, García-Hinojosa JA, Gómez FJR, Mejia-Sintillo S, Salinas-Bravo VM, Lopes-Sesenez R, Gonzalez-Rodriguez JG, Garcia-Pérez CA. Corrosion Behavior of A356/SiC Alloy Matrix Composites in 3.5% NaCl Solution. Int J Electrochem Sci, 2019; 14:7423-7436. https://doi.org/10.20964/2019.08.33
[29] Sambathkumar M, Gukendran R, Mohanraj T, Karupannasamy DK, Natarajan N, Christopher DS. A Systematic Review on the Mechanical, Tribological, and Corrosion Properties of Al 7075 Metal Matrix Composites Fabricated through Stir Casting Process. Advances in Materials Science and Engineering 2023. https://doi.org/10.1155/2023/5442809
[30] Abdulwahab M, Dodo R, Suleiman I, Gebi A, Umar I. Wear behavior of Al-7%Si-0.3%Mg/melon shell ash particulate composites. Heliyon. 2017 Aug;3(8):e00375. https://doi.org/10.1016/j.heliyon.2017.e00375
[31] Sanusi KO, Alaneme KK. Microstructural characteristics, mechanical and wear behavior of aluminum matrix hybrid composites reinforced with alumina, rice husk ash and graphite. Engineering Science and Technology, an International Journal, 2015; 18:416-422. https://doi.org/10.1016/j.jestch.2015.02.003
[32] Mishra P, Mishra P, Rana R. Effect of Rice Husk ash Reinforcements on Mechanical properties of Aluminium alloy (LM6) Matrix Composites. Materials Today: Proceedings. 2018;5(2):6018-22. https://doi.org/10.1016/j.matpr.2017.12.205
[33] Oke SR, Bayode A, Falodun OE, Olasupo IS. Microstructure, mechanical, and wear properties evaluation of Al-Cu based composite using RHA as reinforcement. Canadian Metallurgical Quarterly. 2025 Apr 3;64(2):396-405. https://doi.org/10.1080/00084433.2024.2357859
[34] Mustafa S, Haider J, Matteis P, Murtaza Q. Synthesis and Wear Behaviour Analysis of SiC- and Rice Husk Ash-Based Aluminium Metal Matrix Composites. J Compos Sci. 2023 Sep 15;7(9):394. https://doi.org/10.3390/jcs7090394
[35] Omoniyi P, Adekunle A, Ibitoye S, Olorunpomi O, Abolusoro O. Mechanical and microstructural evaluation of aluminum matrix composite reinforced with wood particles. Journal of King Saud University - Engineering Sciences. 2022; 34:445-450. https://doi.org/10.1016/j.jksues.2021.01.006
[36] Abolusoro OP, Khoathane MC, Washington W. Mechanical and microstructural characteristics of recycled aluminum matrix reinforced with rice husk ash. AIMS Materials Science 2024; 11:918-934. https://doi.org/10.3934/matersci.2024044
[37] Aydın F. A review of recent developments in the corrosion performance of aluminium matrix composites. Journal of Alloys and Compounds. 2023 Jul;949:169508. https://doi.org/10.1016/j.jallcom.2023.169508
[38] Elijah OA, Akinlabi ET, Jen TC, Oladijo PO, Olorunfemi TR, Abolusoro O. Investigation of orange peel as an inhibitor on the corrosion susceptibility of mild steel. In: AIP Conference Proceedings. American Institute of Physics. 2024. https://doi.org/10.1063/5.0215687
[39] Yasakau KA, Zheludkevich ML, Ferreira MGS. Role of intermetallics in corrosion of aluminum alloys. Smart corrosion protection. In: Intermetallic Matrix Composites: Properties and Applications. Elsevier, 2018; 425-462. https://doi.org/10.1016/B978-0-85709-346-2.00015-7
[40] Ikeuba AI, Njoku CN, Ekerenam OO, Njoku DI, Udoh II, Daniel EF, Uzoma PC, Etim IIN, Okonkwo BO. A review of the electrochemical and galvanic corrosion behavior of important intermetallic compounds in the context of aluminum alloys. Royal Society of Chemistry Advances, 2024; 14:31921-31953. https://doi.org/10.1039/D4RA06070A
[41] Parangusan H, Bhadra J, Al-Thani N. A review of passivity breakdown on metal surfaces: influence of chloride- and sulfide-ion concentrations, temperature, and pH. Emergent Materials. 2021; 4 (2) 1-17. https://doi.org/10.1007/s42247-021-00194-6
[42] Barbucci A, Bruzzone G, Delucchi M, Panizza M, Cerisola G. Breakdown of passivity of aluminum alloys by intermetallic phases in neutral chloride solution. Intermetallics,. 2000; (8), 3; 305-312. https://doi.org/10.1016/S0966-9795(99)00114-4
[43] Bodunrin M, Alaneme KK, Ademilua BO, Bodunrin MO, Alaneme KK. Mechanical Properties and Corrosion Behavior of Aluminum Hybrid Composites Reinforced with Silicon Carbide and Bamboo Leaf Ash. Tribology in Industry, 2013; 35 (1): 25-35.

[44] Fangmin Shen, Guojian Liu, Cheng Liu, Yunsheng Zhang, Lin Yang. Corrosion and oxidation on iron surfaces in chloride-contaminated electrolytes: Insights from ReaxFF molecular dynamic simulations. Journal of Materials Research and Technology, 2024; 29:1305-1312. https://doi.org/10.1016/j.jmrt.2024.01.194
[45] O'Grady WE, Roeper DF, Natishan PM. Structure of chlorine K-edge XANES spectra during the breakdown of passive oxide films on aluminum. Journal of Physics Chem. C 115. 2011; 51:25298-25303. https://doi.org/10.1021/jp2056305
[46] Rui X, Quantong J, Chang L, Xinhe W, Yahui G, Jizhou D, Baorong H. The microstructure and corrosion characteristics of Al-10 wt % RE (Re= Ce, Nd, La, Y) binary aluminum alloys in natural seawater. Journal of Materials Research and Technology. 2024; (33): 6408-6421. https://doi.org/10.1016/j.jmrt.2024.11.007
[47] Bangalore Gangadharacharya Koushik, Nils Van den Steen, Mesfin Haile Mamme, Yves Van Ingelgem, Herman Terryn. Review on modelling of corrosion under droplet electrolyte for predicting atmospheric corrosion rate. Journal of Materials Science & Technology. 2021; 62: 254-267. https://doi.org/10.1016/j.jmst.2020.04.061
[48] Yahui Wang, Jingjing Zhang, Weiqiang Wang, Fengyun Yu, Weisheng Cao, Shuhai Hu. Effect of sodium fluoride additive on microstructure and corrosion performance of micro-arc oxidation coatings on EK30 magnesium alloy. Surface and Coating Technology. 2025; 496. https://doi.org/10.1016/j.surfcoat.2024.131628
[49] Abolusoro OP, Akinlabi ET. Effects of processing parameters on mechanical, material flow and wear behavior of friction stir welded 6101-T6 and 7075-T651 aluminum alloys. Manufacturing Review 2020; 7:1-14. https://doi.org/10.1051/mfreview/2019026
[50] Noder J, George R, Butcher C, Worswick MJ. Friction characterization and application to warm forming of a high-strength 7000-series aluminum sheet. J Material Process Technology,2021;293:117066. https://doi.org/10.1016/j.jmatprotec.2021.117066
[51] Dada M, Popoola P. Recent advances in joining technologies of aluminum alloys: a review. Discover Materials, 2024; 4, 86. https://doi.org/10.1007/s43939-024-00155-w
[52] Awad AY, Ibrahim MN, Hussein MK. Effects of Rice Husk Ash-Magnesium Oxide Addition on Wear Behavior of Aluminum Alloy Matrix Hybrid Composites. Tikrit Journal of Engineering Sciences, 2018; 25:16-23. https://doi.org/10.25130/tjes.25.4.04
[53] Indumathi M, Nakkeeran G, Roy D, Gupta SK, Alaneme GU. Innovative approaches to sustainable construction: a detailed study of rice husk ash as an eco-friendly substitute in cement production. Discov Appl Sci. 2024 Nov 9;6(11):597. https://doi.org/10.1007/s42452-024-06314-1
[54] Shanmughasundaram P, Subramanian R. Wear behavior of eutectic Al-Si alloy-graphite composites fabricated by combined modified two-stage stir casting and squeeze casting methods. Advances in Materials Science and Engineering 2013. https://doi.org/10.1155/2013/216536